Molecular Dynamics Simulation of Amyloid β Dimer Formation

B. Urbanc,* L. Cruz,* F. Ding,*† D. Sammond,† S. Khare,† S. V. Buldyrev,* H. E. Stanley,* and N. V. Dokholyan†

*Center for Polymer Studies, Department of Physics, Boston University, Boston, Massachusetts; and †Department of Biochemistry and Biophysics, University of North Carolina at Chapel Hill, School of Medicine, Chapel Hill, North Carolina

ABSTRACT Recent experiments with amyloid β (Aβ) peptide indicate that formation of toxic oligomers may be an important contribution to the onset of Alzheimer's disease. The toxicity of Aβ oligomers depends on their structure, which is governed by assembly dynamics. Due to limitations of current experimental techniques, a detailed knowledge of oligomer structure at the atomic level is missing. We introduce a molecular dynamics approach to study Aβ dimer formation. 1), We use discrete molecular dynamics simulations of a coarse-grained model to identify a variety of dimer conformations; and 2), we employ all-atom molecular mechanics simulations to estimate thermodynamic stability of all dimer conformations. Our simulations of a coarse-grained Aβ peptide model predicts 10 different planar β-strand dimer conformations. We then estimate the free energies of all dimer conformations in all-atom molecular mechanics simulations with explicit water. We compare the free energies of Aβ(1–42) and Aβ(1–40) dimers. We find that 1), dimer conformations have higher free energies compared to their corresponding monomeric states; and 2), the free-energy difference between the Aβ(1–42) and the corresponding Aβ(1–40) dimer conformation is not significant. Our results suggest that Aβ oligomerization is not accompanied by the formation of thermodynamically stable planar β-strand dimers.

INTRODUCTION

Alzheimer's disease (AD) is neuropathologically characterized by progressive neuronal loss, extracellular amyloid plaques, and intracellular neurofibrillary tangles (Yankner, 1996; Selkoe, 1997). Fibrillar amyloid plaques, a result of amyloid β (Aβ) peptide aggregation, have been implicated in the pathogenesis of AD. Recent experimental studies on Aβ peptide (Lambert et al., 1998; El-Agnaf et al., 2000, 2001; Dahlgren et al., 2002) as well as various animal model studies (Hsia et al., 1999; Mucke et al., 2000; Dodart et al., 2002; Westerman et al., 2002; Walsh et al., 2002) suggest that soluble forms of Aβ assemblies cause substantial neuronal dysfunction even before the appearance of amyloid plaques. Hence, finding the conformation of these oligomeric forms of Aβ may be important for understanding of neurotoxicity in AD (Kirkitadze et al., 2002; Klein et al., 2001; Klein, 2002a,b; Bucciantini et al., 2002; Kayed et al., 2003). At present, the precise nature, conformation, and time evolution from monomer Aβ peptides into intermediates is still unknown.

The fibrillar structure of Aβ peptide aggregates is relatively well established. Experiments have targeted the structure of Aβ fibrils using electron microscopy (Malinchik et al., 1998; Tjernberg et al., 1999, 2002), x-ray diffraction (Malinchik et al., 1998; Serpell et al., 2000), electron paramagnetic resonance spectroscopy (Török et al., 2002) and solid-state NMR spectroscopy (Balbach et al., 2002; Petkova et al., 2002; Antzutkin et al., 2002, 2003; Thompson, 2003). The most common view is that Aβ(1–40) and Aβ(1–42) in fibrils form parallel β-sheets with a β-turn between residues Asp-23 and Lys-28. The most flexible regions of the peptide in a fibril are the first 10 amino acids of the N-terminus, last few amino acids of the C-terminus (residues 39–42), and the β-turn region between residues 23 and 28 (Petkova et al., 2002; Török et al., 2002).

The aggregation process from a monomer Aβ peptide via soluble oligomeric states to fibrils is a complex dynamic event that depends critically on the peptide concentration, pH, and solvent properties. Structural studies have shown that in vitro, Aβ fibril formation is preceded by formation of intermediates, spherical oligomeric states, and protofibrils (Walsh et al., 1997, 1999; Hartley et al., 1999; Kirkitadze et al., 2001; Yong et al., 2002). Structural studies on oligomeric states are in a less advanced stage compared to those in fibrils. The nature and structure of different oligomeric states may depend crucially on the specific amino acid sequence of the peptide (Nilsberth et al., 2001). The Aβ plaques in AD brain are predominantly comprised of two Aβ alloforms, Aβ(1–40) and Aβ(1–42). Despite the relatively small structural difference between these two alloforms, they display distinct behavior, with Aβ(1–42) being a predominant component of parenchymal plaques (Suzuki et al., 1994; Iwatsubo et al., 1994; Gravina et al., 1995), associated with both early onset AD (Scheuner et al., 1996; Golde et al., 2000) and increased risk for AD (Weggen et al., 2001). The cause of the clinical differences between the two alloforms is still unknown. Recent experiments have shown that in vitro Aβ(1–40) and Aβ(1–42) oligomerize through distinct pathways, with Aβ(1–42) forming spherical paranuclei that further assemble into higher-order oligomers (Bitan et al., 2001, 2003a,b).

Submitted February 2, 2004, and accepted for publication June 1, 2004.

Address reprint requests to B. Urbanc, Center for Polymer Studies, Dept. of Physics, Boston University, Boston, MA 02215. E-mail: brigita@bu.edu.

0006-3495/04/10/2310/12 $2.00

doi: 10.1529/biophysj.104.040980

Several studies found stable soluble Aβ low molecular weight oligomers (Barrow and Zagorski, 1991; Barrow et al., 1992; Zagorski and Barrow, 1992; Soreghan et al., 1994; Shen and Murphy, 1995; Podlisny et al., 1995; Roher et al., 1996; Kuo et al., 1996; Garzon-Rodriguez et al., 1997; Xia et al., 1995; Enya et al., 1999; Funato et al., 1999; Huang et al., 2000). Low molecular weight oligomers were found in culture media of Chinese hamster ovary cells expressing endogenous or mutated genes (Podlisny et al., 1995; Xia et al., 1995). Aβ(1–40) and Aβ(1–42) oligomers, specifically dimers, were isolated from human control and AD brains (Kuo et al., 1996, 1998; Enya et al., 1999; Funato et al., 1999). Dimers and trimers of Aβ were isolated from neuritic and vascular amyloid deposits and dimers were shown to be toxic to neurons in the presence of microglia (Roher et al., 1996). Experiments on synthetic Aβ peptides (Garzon-Rodriguez et al., 1997; Podlisny et al., 1998) showed that soluble Aβ(1–40) exists as a stable dimer at physiological concentrations that are well below the critical micelle concentration (Soreghan et al., 1994).

It has been shown that the β-sheet content of Aβ depends strongly upon the solvent in which the peptide is dissolved (Shen and Murphy, 1995). Various experimental studies (Barrow and Zagorski, 1991; Barrow et al., 1992; Zagorski and Barrow, 1992; Shen and Murphy, 1995) indicate that soluble Aβ has substantial β-sheet content. Huang et al. (2000) reported on two types of soluble oligomers of Aβ(1–40) that were trapped and stabilized for an extended period of time: the first type was a mixture of dimers and tetramers with irregular secondary structure and the second type corresponded to larger spherical particles with β-strand structure. Despite some discrepancies in the experimental results, the studies mentioned above suggest that dimerization may be the initial event in amyloid aggregation and thus dimers may be fundamental building blocks for further fibril assembly.

Experimental methods, such as circular dichroism, NMR, and electron microscopy, provide only limited information on the structure of intermediate oligomeric states. Therefore, there is a motivation to develop new computational approaches to determine the exact conformation of oligomers at the atomic level and track the exact pathway from individual monomer peptides to oligomers and protofibrils in fast and efficient ways. With the dramatic increase of computer power in recent decades, it has become possible to study the behavior of large biological molecular systems by Monte Carlo and molecular dynamics (MD) simulations (Dinner et al., 2002; Fersht and Daggett, 2002; Karplus and McCammon, 2002; Thirumalai et al., 2002; Plotkin and Onuchic, 2002; Mendes et al., 2002; Mirny and Shakhnovich, 2001; Bonneau and Baker, 2001; Dill, 1999; Levitt et al., 1997; Wolynes et al., 1996; Snow et al., 2002; Vorobjev and Hermans, 2001; Zhou and Karplus, 1997). However, traditional all-atom MD with realistic force fields in a physiological solution currently remains computationally unfeasible. An aggregation process as allowed by all-atom MD can only be studied on timescales of up to 10^{-7}s using such advanced technologies as worldwide distributed computing (Snow et al., 2002; Zagrovic et al., 2002). However, in vivo and in vitro studies suggest that the initial stages of oligomerization occur on a timescale of 1 s (Bitan et al., 2003a), whereas further aggregation into protofibrillar and fibrillar aggregates may span hours (Kayed et al., 2003).

Here we conduct a two-step study of Aβ dimer conformations and their stability using a computationally efficient algorithm combined with a coarse-grained peptide model for Aβ. We apply a four-bead model for Aβ peptide to study monomer and dimer conformations of Aβ(1–42) peptide (Ding et al., 2003). We use fast and efficient discrete molecular dynamics (DMD) simulations (Dokholyan et al., 1998; Smith and Hall, 2001a). The DMD method allows us to find and study a large variety of dimer conformations starting from initially separated monomers without secondary structures. Our coarse-grained model combined with the DMD method predicts 10 different planar β-strand dimer conformations. In the second step, we estimate the free energy of Aβ(1–42) and Aβ(1–40) dimeric conformations in a stability study using all-atom MD simulations with explicit water and well-established force fields. This second step enables us to estimate the free energy of different dimeric conformations and to compare the free energies of Aβ(1–42) and Aβ(1–40) for each of the dimer peptides. Our results suggest that Aβ oligomerization is not accompanied by formation of thermodynamically stable planar β-strand Aβ dimers, and that such dimers of both Aβ(1–42) and Aβ(1–40) are equally unlikely to represent thermodynamically stable oligomeric forms.

METHODS

Discrete molecular dynamics simulations

In a DMD simulation, pairs of particles interact by means of spherically symmetric potentials that consist of one or more square wells. Within each well the potential is constant. Consequently, each pair of particles moves with constant velocity until they reach a distance at which the potential changes. At this moment a collision occurs and the two particles change their velocities instantaneously while conserving the total energy, momentum, and angular momentum. There are three main types of collisions. The simplest is when particles collide at their hard-core distance, the sum of the particle radii. In this case, the particles collide elastically, and their kinetic energy before and after the collision is conserved. In the second case, the particles enter a potential well of depth ΔU. In this case, their total kinetic energy after the collision increases by ΔU, their velocities increase, and there is a change in their trajectories. In the third case, particles exit a potential well of depth ΔU. Here, total kinetic energy after the collision decreases by ΔU. If the total kinetic energy of the particles is greater than ΔU, they escape the well. If their total kinetic energy is smaller than ΔU, the particles cannot escape and simply recoil from the outer border of the well inward. At low temperatures, which correspond to low average particle kinetic energies, particles whose potentials are attractive thus have a tendency to remain associated with each other.

DMD, unlike traditional continuous MD, is event-driven and as such it requires keeping track of particle positions and velocities only at collision

times, which have to be sorted and updated. It can be shown that the speed of the most efficient DMD algorithm is proportional to $N \ln N$, where N is the total number of atoms (Rapaport, 1997). In addition, the speed of the algorithm decreases linearly with the number of discontinuities in the potential and particle density. In our DMD simulations the solvent is not explicitly present, which reduces the number of particles in the system. Consequently, the DMD method is several orders of magnitude faster than the traditional continuous MD. The DMD simulation method has been so far successfully applied to simulate protein folding (Zhou and Karplus, 1997; Dokholyan et al., 1998; Ding et al., 2002a; Borreguero et al., 2002) and aggregation (Smith and Hall, 2001a,b; Ding et al., 2002b, 2003). In simulating protein folding and aggregation, coarse-grained models of proteins have been introduced. In a coarse-grain model the number of atoms per amino acid is reduced to one, two, or four, which further speeds up the DMD simulation. Although traditional continuous all-atom MD can simulate events on timescales of nanoseconds, the DMD method combined with a coarse-grained protein model can easily reach timescales of seconds or more, which is long enough to study oligomer formation of up to 100 Aβ peptides.

A coarse-grained model for Aβ peptide

The Aβ peptide is derived from its larger amyloid precursor protein by sequential proteolytic cleavages. In amyloid plaques, the two most common forms of the Aβ peptide are Aβ(1–40) and Aβ(1–42). The amino acid sequence of Aβ(1–42) is DAEFRHDSGYEVHHQKLVFFAEDVGSNK-GAIIGLMVGGVVIA. The amino acid sequence of Aβ(1–40) is the same as that of Aβ(1–42), but shorter by two amino acids at the C-terminus, Ile and Ala. In our approach we build the Aβ peptide model starting from the simplest model, which captures the geometric properties of the peptide backbone and takes into account only intra- and interpeptide hydrogen-bond interactions, which are not amino acid-specific. The advantage of this minimalistic approach is that it will eventually allow us to determine those intra- and interpeptide interactions that are essential for understanding the initial steps in Aβ aggregation process.

The basic amino acid geometry requires that the backbone atoms are represented by at least three ''atoms'' or ''beads.'' In our DMD simulations we apply the four-bead model (Takada et al., 1999; Smith and Hall, 2001a,b; Ding et al., 2003) for Aβ peptide. In this model, each amino acid in the peptide is replaced by at most four ''beads.'' These beads correspond to the atoms comprising the amide nitrogen N, the alpha carbon C_α, and prime-carbon C'. The fourth bead, representing the amino acid side-chain atoms, is placed at the center of the nominal C_β atom. Due to their lack of side chains, the six glycines in Aβ (positions 9, 25, 29, 33, 37, and 38) are represented by only three beads. In effect, in our model the Aβ peptide is a polyalanine chain with glycines. Two beads that form a permanent bond can assume any distance between the minimum and maximum bond length. In addition to permanent bonds between the beads, the model introduces constraints between pairs of beads that do not form permanent bonds. These constraints are implemented to account for the correct peptide backbone geometry. The hard-core radii, minimum and maximum bond lengths, constraints' lengths, and their corresponding standard deviations are either calculated from distributions of experimental distances between pairs of these groups found in ~7700 folded proteins with known crystal structures (Protein Data Bank), or chosen following the standard knowledge of the geometry of the peptide backbone (Creighton, 1993). The values of all these parameters have been reported previously (Ding et al., 2003).

To account for the hydrogen bonding that normally occurs in proteins between the carbonyl oxygen of one amino acid and the amide hydrogen of another amino acid, the coarse-grained model implements a bond between the nitrogen of the ith amino acid, N_i, and the carbon of the jth amino acid, C'_j, as introduced previously (Ding et al., 2003). The planar geometry of the hydrogen bond is modeled by introducing auxiliary bonds between the left and the right neighboring beads of N_i and C'_j. The hydrogen bond between N_i and C'_j will form only if all six beads are at energetically favorable distances. Once the hydrogen bond is formed, it can break due to thermal fluctuations, which can cause energetically unfavorable distances among the six beads involved in the hydrogen bond. When amino acids i and j belong to the same peptide, they can form a hydrogen bond only if at least three amino acids exist between them (to satisfy the 180° NH-CO bond angle). A more detailed description of the hydrogen bond implementation has been given elsewhere (Ding et al., 2003). Our current implementation differs slightly from before (Ding et al., 2003): one of the auxiliary bonds, namely the auxiliary bond between N_i and the bead N (the nearest neighbor of C'_j), has a shorter equilibrium distance: instead of 5.10 ± 0.31 Å used previously (Ding et al., 2003), it is 4.70 ± 0.08 Å. This slight change in the auxiliary bond length stabilizes the β-hairpin monomer conformation in our model as described in the results section.

All-atom molecular dynamics in an explicit solvent

Next we detail how we use all-atom MD simulations in an explicit solvent to compute the conformational free energy of Aβ(1–40) and Aβ(1–42) monomer and dimer conformations.

Preparation of peptide conformations

For Aβ(1–40) monomer peptide structures we use 10 NMR structures with coordinates (Coles et al., 1998) (ID code name 1BA4 of Protein Database Bank). For each of these 10 Aβ(1–40) monomer structures, we construct a corresponding Aβ(1–42) monomer structure by adding two residues, Ile and Ala, to the C-terminus of the peptide using the SYBYL (Tripos, St. Louis, MO) molecular modeling package.

All Aβ(1–42) dimer conformations in this study are generated by DMD simulations using the four-bead model as described above. Dimer conformations, initially in the four-bead representation, are converted into all-atom representation by using all-atom template amino acids. These templates are superposed onto the coarse-grained amino acids such that the four beads of the coarse-grained model coincide with the N, C_α, C', and C_β groups of the all-atom template amino acids. The new template coordinates with increased number of degrees of freedom are optimized for preserving backbone distances as well as formation of peptide planes. This optimization is performed by rotating the template amino acid along two axes, the C_α-N and the C'-C_α axes, using a Monte Carlo algorithm. After positioning the backbone atoms, the positions of side-chain atoms are determined by avoiding steric collisions with the backbone and other neighboring residues. Positioning of side-chain atoms also follows a Monte Carlo algorithm, during which side-chain atoms are rotated sequentially along the C_α-C_β axis and the C_β-C_γ axis to find the optimal combinations of axis angles that prevent collisions. The backbone structure of the resulting peptide remains very close to the initial structure of the peptide: the lengths of bonds and constraints after the conversion are within the limits given by our coarse-grained model and the root mean square displacement between the starting four-bead and the final all-atom conformation is <0.5 Å in all cases. The Aβ(1–40) dimer conformations corresponding to each Aβ(1–42) dimer are constructed by disposing of the last two amino acids of each Aβ(1–42) dimer conformation.

Calculation of the conformational free energy in water

We estimate conformational free energies of monomers and dimers in a water environment using all-atom MD simulations. All MD calculations are performed using the Sigma MD program (Hermans et al., 1994) with CEDAR force fields (Ferro et al., 1980; Hermans et al., 1984). We complete the all-atom reconstruction from above by adding hydrogen atoms and solvating the peptide(s) in an SPC water model bath (Berendsen et al., 1981).

Aβ peptides are capped by acetyl and N-methyl groups at the N- and C-terminals, respectively. We use periodic boundary conditions on a cubic box whose sides extended 12 Å beyond the leading edge of the peptide(s) on all sides. The MD method consists of two stages, equilibration and production (Vorobjev et al., 1998; Vorobjev and Hermans, 1999, 2001; Leach, 2001). Equilibration allows both the peptides and water to relax to a local energy minimum. The steps of equilibration, 1–7, and the production step, 8, are as follows:

1. Minimize the energy of the water—peptides are kept immobile.
2. Perform MD simulations on the water using the NVT ensemble at a temperature $T = 200$ K for 96 ps (the time step is 1 fs)—peptides are kept immobile.
3. Minimize the energy of the water a second time—peptides are kept immobile.
4. Minimize the energy of the peptides—water molecules are kept immobile.
5. Perform MD simulations of the peptide using the NVT ensemble at a temperature ($T = 100$ K)—water molecules are kept immobile.
6. Minimize the energy of the peptides a second time—water molecules are kept immobile.
7. Minimize the energy of the peptides and water molecules simultaneously.
8. Perform the production run, i.e., unconstrained MD simulations on the peptides and water using the NPT ensemble at $T = 300$ K and $P = 1$ atm for 196 ps.

At steps 1, 3, 4, 6, and 7 we use the steepest descent energy minimization method. During steps 2 and 5, which are parts of equilibration, peptide(s) and water coordinates have to reach a local energy minimum for the given force field and with respect to each other. The temperatures are kept low so that there are no conformational changes.

During the production run, step 8, we maintain constant temperature and pressure by Berendsen coupling (Berendsen et al., 1984) and calculate electrostatic forces using the particle-mesh Ewald procedure (Darden et al., 1993). We record a snapshot of the configuration every picosecond. We calculate the free energy for each conformation by averaging the instantaneous free energy for each of the 196 snapshots. Each of these snapshots represents a microconfiguration. We calculate the free energy for each configuration by the ES/IS method (Vorobjev and Hermans, 1999), which uses an explicit solvent simulation with an implicit solvent continuum model:

$$G_{\mathrm{A}} = \langle U_{\mathrm{m}}(x)\rangle_{\mathrm{A}} + \langle W(x)\rangle_{\mathrm{A}} - TS_{\mathrm{conf,A}}, \qquad (1)$$

where $\langle \ldots \rangle_{\mathrm{A}}$ denotes an average over all recorded microconfigurations of the conformation A, U_{m} is the intraprotein conformational energy, and $S_{\mathrm{conf,A}}$ is the entropy of conformation A. The intraprotein conformational energy, U_{m}, is a sum of two terms: one is the short-range energy of packing, $U_{\mathrm{m,pack}}$, and the other is the electrostatic energy due to coulombic interactions, $U_{\mathrm{m,coul}}$. The solvation free energy, $W(x)$, is the sum of three terms: the first one, G_{cav}, is the energy required to form a cavity in the solvent; the second one, $G_{\mathrm{s,vdw}}$, is a contribution of the van der Waals interactions between solvent and protein; and the third one, G_{pol}, is a contribution of the electrostatic polarization of the solvent and polar components of the solute. Thus the above equation becomes

$$G_{\mathrm{A}} = \langle U_{\mathrm{m,pack}}\rangle_{\mathrm{A}} + \langle U_{\mathrm{m,coul}}\rangle_{\mathrm{A}} + \langle G_{\mathrm{cav}}\rangle_{\mathrm{A}} + \langle G_{\mathrm{s,vdw}}\rangle_{\mathrm{A}} + \langle G_{\mathrm{pol}}\rangle_{A} - TS_{\mathrm{conf,A}}. \qquad (2)$$

We determine U_{m} and $G_{\mathrm{s,vdw}}$ from the MD trajectory, calculate G_{cav} as proportional to the accessible surface area for a given microconfiguration, and evaluate G_{pol} using an implicit model for the solvent as described elsewhere (Vorobjev and Hermans, 1999).

RESULTS

Characterization of monomer conformations

The secondary structure of both Aβ(1–40) and Aβ(1–42) monomer peptides, as determined by NMR conformational studies in an apolar environment that mimics the lipid phase of membranes, is predominantly α-helical. Two α-helical regions exist at residues 8–25 and 28–38, and these regions are separated by a flexible hinge. The rest of the peptide adopts random coil-like conformation (Coles et al., 1998; Crescenzi et al., 2002).

To characterize the monomer conformations in our coarse-grained model, we calculate an average potential energy in dependence on the temperature. The energy unit corresponds to the potential energy of one hydrogen bond in our model, so that the absolute average of the potential energy is equal to the average number of hydrogen bonds in the monomer conformation, and the temperature unit is equal to the energy unit. At each temperature $0.080 < T < 0.155$, we perform 35×10^6 time step-long simulations. We start each run with an initial conformation equal to the observed NMR conformation with predominantly α-helical secondary structure (Crescenzi et al., 2002). The first 15×10^6 steps we allow for equilibration, whereas we calculate the time average of the potential energy $\langle E\rangle$ over the last 20×10^6 time steps.

Our monomer peptide experiences a structural transition from a predominantly α-helix conformation into a β-strand conformation at $T_{\alpha,\beta} = 0.107 \pm 0.002$, in agreement with previous work (Ding et al., 2003). At a higher temperature, $T_{\beta,\mathrm{RC}} = 0.128 \pm 0.002$, the monomer undergoes a transition from a β-strand into a random-coil conformation with no particular secondary structure. Between $T_{\alpha,\beta}$ and $T_{\beta,\mathrm{RC}}$ our simulations show various types of β-strand rich conformations.

At temperatures $T < 0.107$, we observe an α-helix conformation, which is consistent with the observed solution monomer conformation in an apolar microenvironment (Crescenzi et al., 2002). This conformation (Fig. 1 *a*) has a random coil-like tail ~10 amino acids long at the N-terminus and another random coil-like tail ~2–4 amino acids long at the C-terminus. At residues 11–40 there are two α-helices, separated by a hinge at residues 25–28. The average potential energy of this conformation is $\langle E\rangle = -28 \pm 2$. At temperatures $0.107 < T < 0.117$, we observe various β-strand conformations, mostly with two or three β-turns, corresponding to three or four β-strands (Fig. 1, *b* and *c*). The average potential energy of these conformations is $\langle E\rangle = -17 \pm 1$. The β-hairpin conformation, i.e., a 2-β-strand conformation with one β-turn, shown in Fig. 1 *d*, is found as a predominant conformation at temperatures T, $0.117 < T < 0.126$. This conformation is characterized by a random-coil tail at residues 1–9 and by a well-defined and localized β-turn which is positioned at residues 23–28. The average potential energy of this conformation is $\langle E\rangle = -13 \pm 1$.

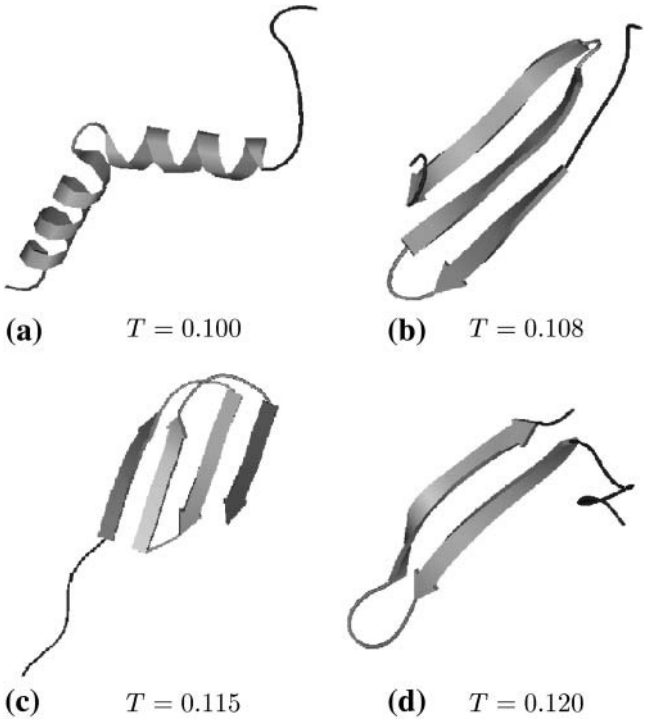

FIGURE 1 Conformations of an Aβ(1–42) monomer peptide model as a function of temperature: (*a*) mostly α-helix conformation at $T = 0.100$ with two α-helices at residues 12–23 and 29–38, and a hinge at residues 23–28; (*b*) 3-β-strand conformation at $T = 0.108$; (*c*) 4-β-strand conformation at $T = 0.115$; and (*d*) β-hairpin conformation at $T = 0.120$ characterized by a β-turn at residues 23–28.

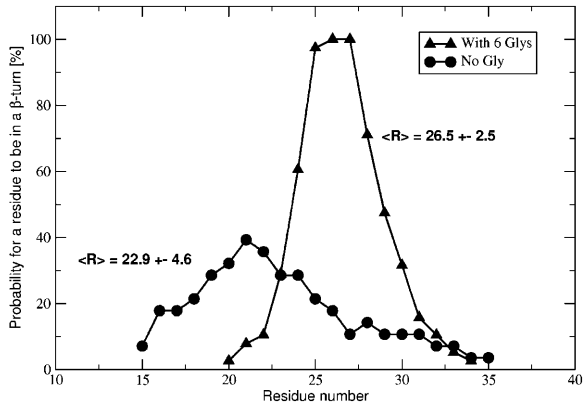

FIGURE 2 Two distributions that give the probability for an amino acid at a residue number (position in the chain) to be within a β-turn. These simulations are done at temperature $T = 0.125$, where our model for Aβ(1–42) yields a stable β-hairpin conformation. The curve with solid circles corresponds to the altered chain (no glycines) and the curve with solid triangles corresponds to the original Aβ(1–42) model with six glycines. The distributions are calculated on the basis of 28 (the model with no glycines) and 38 (the Aβ(1–42) model) different β-hairpin configurations. For each β-hairpin conformation we use a visual molecular dynamics (VMD) (Humphrey et al., 1996) visualization package to determine and count all the residues with a β-turn (determined visually and confirmed by the secondary-structure analysis within VMD). The probability to be in the β-turn is determined as a ratio between the number of conformations in which the amino acid is part of a β-turn and the total number of conformations.

The observed β-turn between residues Asp-23 and Lys-28 is in agreement with recent NMR studies of Aβ fibrillar structure (Petkova et al., 2002). In the following, we provide an empirical explanation for the occurrence of this well-defined β-turn in our model. We hypothesize that within our model the occurrence of a β-turn at residues 23–28 is induced by the particular location of the six glycines in the Aβ(1–42) peptide. To test this hypothesis, we replace all glycines within the Aβ(1–42) peptide with alanines and perform simulations as described above. Our results (Fig. 2) show the probability for the amino acid at a certain position to be part of a β-turn both for the original Aβ peptide model (with glycines) and the one without glycines (42 amino acid-long polyalanine chain). The results show that 1), the presence of glycines on average shifts the center of the β-turn from residues 20–22 for the chain with no glycines to 25–27 for the chain with six glycines, and 2), the probability distribution in the presence of glycines is strongly peaked at residues 25–27, which makes these three residues part of the β-turn with >95% probability, and thus the β-turn is well-defined.

The residues 25–27 of the Aβ peptide correspond to glycine, serine, and asparagine, the residues that have, according to the classical phenomenological approach of Chou and Fasman (1974), the highest probability to be within a β-turn. In our coarse-grained model the occurrence of the β-turn at 23–28 can be understood as a consequence of two tendencies: 1), a tendency to maximize the number of hydrogen bonds, which prefers a β-turn at the middle of the peptide chain, centered at resides 20–22; and 2), a tendency of six glycines to be associated with more flexibility, thus a β-turn. Consequently, the center of the β-turn is shifted from residues 20–22 to residues 25–27 and is well-defined.

Planar β-strand dimer conformations of Aβ(1–42)

We investigate next dimer formation of Aβ(1–42) peptides. The initial monomer conformations are taken from the Protein Data Bank and correspond to the observed NMR structures of Aβ(1–42) monomers in an apolar environment (Crescenzi et al., 2002). To obtain different starting random-coil conformations, we place two monomers with mostly α-helical secondary structure in a cubic box with a side length of 100 Å. The centers of masses of the two monomers are initially ~50 Å apart and their orientations parallel. Next, we heat the system up to a temperature $T = 0.50$, which is far above the observed $T_{\beta,\mathrm{RC}}$ temperature. The α-helical secondary structure of individual monomer peptides is dissolved in ~200 simulation steps, producing two peptides with different random-coil conformations. We use many similarly generated pairs of peptides with random-coil conformations as initial configurations in our study of dimer formation. Dimer formation simulations are done at a constant

temperature and volume. We perform 20 simulations at a fixed temperature. Each run is 20×10^6 time steps long. In this way we explore temperatures $T = 0.120$, 0.125, and 0.130.

From the above simulations we find six possible dimer conformations with the following characteristics: 1), each peptide in a dimer is in a β-hairpin conformation with two β-strands; and 2), all four β-strands (two per peptide) are planar. We name those dimers according to the inner two strands of the dimer (each strand is closer to either the N-terminus or the C terminus and the two inner strands are either parallel or antiparallel): NN-parallel, NC-parallel, CC-parallel, NN-antiparallel, NC-antiparallel, and CC-antiparallel. These conformations are schematically presented in Fig. 3, *a–f*. We find four additional dimer conformations with characteristic 2 described above. Only the inner peptide has also characteristic 1, whereas the outer peptide is bent around the inner one, forming a ''nest.'' We term them nested-parallel, nested-antiparallel, anti-nested parallel, and anti-nested antiparallel (in anti-nested conformations the termini of the two peptides are in the opposite directions). They are shown in Fig. 3, *g–j*.

At $T = 0.12$, we find NC-parallel and NC-antiparallel conformations in 3 out of 20 simulations. The conformations NN-parallel, CC-parallel, CC-antiparallel, nested antiparallel, anti-nested parallel, and anti-nested antiparallel each occur in 2 out of 20 simulations. The conformations NN-antiparallel and nested parallel are each found in 1 out of 20 simulations. At $T = 0.13$, the most common dimer peptide conformation is NC-parallel (occurring in 8 out of 20 simulations) and the next most common conformation is NN-parallel (occurring in 5 out of 20 simulations). We find the NC-antiparallel conformation in 3 out of 20 simulations. There are four more conformations found, each in 1 out of 20 simulations: NN-antiparallel, CC-parallel, CC-antiparallel and a nested-antiparallel conformation.

Our dimer simulations at temperatures $T \geq 0.14$ show no dimerization within the first 20×10^6 simulation steps, even though typically one of the two peptides adopts one of the β-strand conformations. We thus conclude that at temperatures $T > 0.14$ there is no dimerization. At temperature $T = 0.11$, we observe a large number of different planar and non-planar β-strand dimer conformations, which are a mixture of

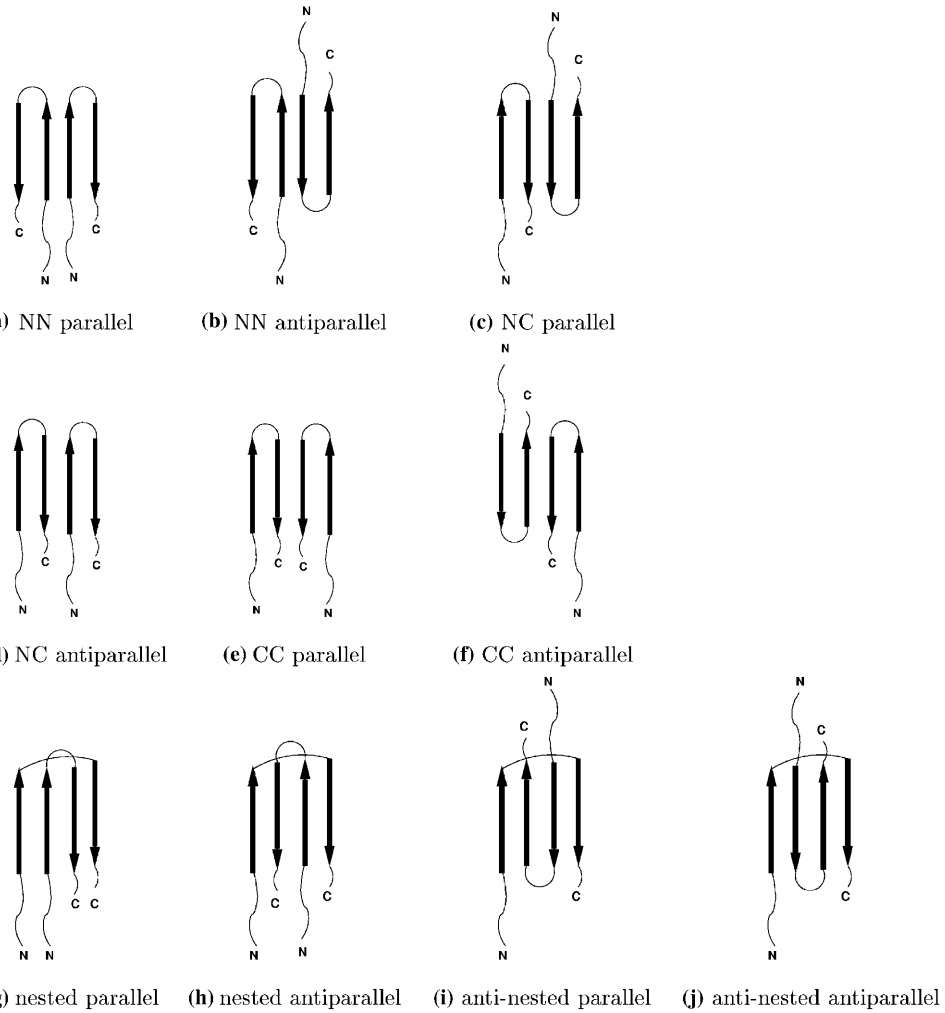

FIGURE 3 Schematic conformations of an Aβ(1–42) dimer peptide model. All the conformations are based on a β-hairpin conformation with a β-turn at residues 23–28. In our model the energies of all these conformations are approximately the same; however, the probability of the occurrence varies.

2-, 3-, and 4-β-strand conformations. At temperatures $0.08 < T < 0.11$, the dimer conformations are an amorphous mixture of β-strand and α-helical secondary structure. All these are omitted from the present all-atom free-energy calculation study.

Free-energy calculations: Aβ(1–40) versus Aβ(1–42) monomer conformations

We first calculate the conformational free energies of monomer peptides of Aβ(1–40) and Aβ(1–42). We choose 10 different NMR Aβ(1–40) monomer structures (Coles et al., 1998). The secondary monomer structure is mostly α-helical, similar to Fig. 1 *a*. These monomer structures were determined under the same experimental conditions, so their conformational free energies should be similar. To each of these structures we add two amino acids, Ile and Ala, to find the corresponding Aβ(1–42) monomer conformation. The estimated free energies are presented in Table 1. Our results show that all the monomer conformations of Aβ(1–40) and Aβ(1–42) have on average the same conformational free energy, -1034.68 ± 17.75 kcal/mol and -1029.47 ± 10.80 kcal/mol, respectively. Each of the two error bars, 17.75 kcal/mol and 10.80 kcal/mol, is a result of averaging over 10 monomer conformations with free energies, given in Table 1. These results show that addition of two amino acids to the C-terminus does not alter the conformational free energy of the Aβ monomer peptide in a water environment at physiological conditions.

Stability analysis of Aβ(1–40) and Aβ(1–42) dimer conformations

The planar β-strand dimer conformations predicted by our coarse-grained model (Fig. 3) are tested for stability in our all-atom MD simulations in an explicit water environment at atmospheric pressure and room temperature. From 10 different Aβ(1–42) dimer conformations, we create the corresponding Aβ(1–40) dimers by deleting the last two amino acids at the C-terminus. For each mechanically stable dimer configuration, we next calculate the free energy as described in the Methods section. The final free energies of all mechanically stable dimers are presented in Table 2. One dimer conformation, e.g., nested antiparallel of Aβ(1–40), is determined to be mechanically only marginally stable and does not allow for the free-energy calculation.

TABLE 1 Free energies of monomer conformations: comparison of calculated free energies, $G_{A\beta-40}$ and $G_{A\beta-42}$, and the corresponding standard deviations, σ_G, of Aβ monomer conformations as determined by the NMR experiment

Monomer	$G_{A\beta-40}$	σ_G	$G_{A\beta-42}$	σ_G
1BA4-01	−1036.58	24.39	−1026.23	24.99
1BA4-02	−1050.25	22.60	−1034.13	22.92
1BA4-03	−1045.88	23.32	−1028.07	21.58
1BA4-04	−1045.93	22.72	−1032.92	30.42
1BA4-05	−1030.62	23.01	−1008.66	25.46
1BA4-06	−997.14	23.11	−1017.85	26.97
1BA4-07	−1043.71	24.26	−1039.30	22.91
1BA4-08	−1016.94	22.70	−1027.37	24.15
1BA4-09	−1038.70	23.16	−1032.68	22.03
1BA4-10	−1052.29	25.82	−1044.28	19.82

The NMR experiment data are based on work of Coles et al. (1998). The names of different monomer structures follow the ID code name 1BA4 of Brookhaven Protein Data Bank (http://www.rcsb.org/pdb/). The free-energy unit is kcal/mol.

Tables 3 and 4 give details of the free-energy calculation for Aβ(1–40) and Aβ(1–42) dimers: individual terms of the free energy with the corresponding error bars. During 200 picosecond-long production runs, we sample each individual contribution to the free energy every picosecond. Thus, we obtain histograms of all the contributions to the free energies, each consisting of 200 data points. We estimate the error bars of each individual term and the total free energy as standard deviations (widths of the corresponding histograms). The entropy term is not included in Tables 3 and 4 as it varies negligibly from trajectory to trajectory. Note that standard deviations of individual contributions to the free energy (Tables 3 and 4) are larger than error bars of the total conformational free energy (Table 2), because these individual contributions are anticorrelated. With an exception of one Aβ(1–40) dimer, for all the rest of dimer conformations the free-energy terms (Tables 3 and 4) are all well-behaved, indicating that these conformations are realistic, i.e., mechanically stable in water. Considering the solvation free energy, which is determined as a sum of three free-energy contributions, $\langle G_{cav}\rangle_A$, $\langle G_{s,vdw}\rangle_A$, and $\langle G_{pol}\rangle_A$ (columns 3, 4, 5, and 6 of Tables 3 and 4), is negative for all mechanically stable dimers, suggesting that all these dimer structures are soluble in water. An evidence that our coarse-grained model dimers are not unrealistic is presented in Fig. 4 which shows the root mean square displacement (RMSD) during the production run for two representative Aβ(1–40) dimers, NN-anti, and CC-anti. RMSDs increase at the beginning of the production run, but stabilize typically after 100 ps at 2–4 Å.

Columns 3 and 6 of Table 2 represent the free-energy differences, $\Delta G_{A\beta\text{-}40}$ and $\Delta G_{A\beta\text{-}42}$, between a dimer conformation and two monomer conformations. For the conformational free energy of the Aβ(1−40) and Aβ(1–42) monomer, we take the averages -1034.68 ± 17.75 kcal/mol and -1029.47 ± 10.80 kcal/mol (see the previous subsection). For two Aβ(1–40) dimers (NN-anti and CC-anti), the difference in the free energy (ΔG) between dimer and monomers (10.52 and 27.91 kcal/mol) is significantly smaller than the quadrature uncertainty in free-energy estimates (46.94 kcal/mol). This suggests that these structures may be marginally thermodynamically stable. However, because for 19 out of 20 dimer conformations ΔG is positive (see Table 2), we conclude that in a water environment, planar β-strand dimer conformations are energetically unfavorable compared to α-helical monomer

TABLE 2 Free energies of dimer conformations: comparison of calculated free energies $G_{A\beta-40}$ and $G_{A\beta-42}$, the corresponding standard deviations σ_G, and the free-energy differences $\Delta G_{A\beta-40}$ and $\Delta G_{A\beta-42}$ of Aβ(1–42) and Aβ(1–40) dimer conformations

Dimer	$G_{A\beta-40}$	σ_G	$\Delta G_{A\beta-40}$	$G_{A\beta-42}$	σ_G	$\Delta G_{A\beta-42}$
NN-para	−1983.51	29.32	88.10	−1994.72	35.03	63.58
NN-anti	−2061.09	34.70	10.52	−2019.14	38.16	39.15
NC-para	−1935.59	32.43	136.02	−1937.60	28.65	120.70
NC-anti	−1999.38	30.77	72.23	−1982.94	40.80	75.36
CC-para	−2000.17	30.36	71.44	−1871.82	30.13	186.48
CC-anti	−2043.70	34.24	27.91	−2022.44	35.77	35.86
nest-para	−1964.90	40.24	106.71	−1989.43	35.05	68.87
nest-anti	N/A	N/A	N/A	−1950.07	45.45	108.23
anti-nest-para	−2028.34	42.19	34.27	−2022.27	30.97	36.03
anti-nest-anti	−1988.27	35.97	83.34	−1972.38	33.80	85.92

The free-energy unit is kcal/mol.

peptide conformations, and thus thermodynamically most likely unstable. Comparing conformational free energies of Aβ(1–40) and Aβ(1–42) dimers, we find that the average conformational free energies are -2000.81 ± 46.94 kcal/mol and -1967.63 ± 52.85 kcal/mol, respectively. Although Aβ(1–40) dimers have on average lower conformational free energy than Aβ(1–42) dimers, the difference is not statistically significant.

DISCUSSION AND CONCLUSIONS

In this work, we introduce a molecular dynamics approach that combines DMD simulations of a coarse-grained Aβ peptide model with all-atom molecular mechanics study of thermodynamic stability of predicted dimer conformations. In our simple coarse-grained peptide model, Aβ peptide is a polyalanine chain with glycines. The model only considers intra- and interpeptide hydrogen bond interactions. Because the model neglects the amino acid-specific interactions, it is in the present form not adapted for modeling the membrane environment, where reduced dimensionality and hydrophobic interactions are critical. In fact, a theoretical model of ion channel structure of Aβ (Durell et al., 1994) is very different from the dimer structures predicted by our coarse-grained model. Our model is thus most pertinent to oligomer formation in solution.

Different dimer conformations, predicted by our coarse-grained model, are transformed into all-atom representations by restoring the specific side chains of Aβ peptides. To study stability of dimer conformations, we apply the all-atom ES/IS method with realistic force fields (Vorobjev and Hermans, 1999) to estimate the free energy of predicted dimer conformations. Within the ES/IS method, a particular source of error in the conformational free-energy calculation arises from applying the implicit solvation method to determine the solvation free energy, which is typically overestimated. Despite limitations, the ES/IS method has been successfully applied to the folding problem: the free energy of misfolded proteins was shown to be higher than the free energy of naturally folded proteins (Vorobjev and Hermans, 2001).

Our results provide the following insights into the nature of Aβ folding and dimer formation. 1), Our model predicts a thermally induced conformational change between a predominantly α-helix to a predominantly β-strand monomer peptide. This prediction of our model, a change from an α-helix-rich to a β-strand-rich monomer conformation, is indirectly supported by recent experiments (Gursky and Aleshkov, 2000) on temperature dependence of the Aβ conformation in aqueous solutions, which suggest that thermally induced conformational change to β-strand transition is not coupled to aggregation and can occur at the level of monomers or dimers. 2) A monomer peptide in

TABLE 3 Individual free-energy terms contributing to the free energy of Aβ-(1–40) dimer conformations ($\langle G_{s,\,vdw}\rangle_A = \langle G_{s,\,vdw,\,6}\rangle_A + \langle G_{s,\,vdw,\,12}\rangle_A$)

Dimers	$\langle U_{m,\,pack}\rangle$	$\langle U_{m,\,coul}\rangle$	$\langle G_{cav}\rangle_A$	$\langle G_{s,\,vdw,\,6}\rangle_A$	$\langle G_{s,\,vdw,\,12}\rangle_A$	$\langle G_{pol}\rangle_A$
NN-para	404.80 (±20.43)	−724.58 (±58.18)	423.46 (±8.31)	−1366.17 (±32.31)	1193.20 (±38.79)	−1914.21 (±51.82)
NN-anti	363.71 (±21.97)	−899.38 (±67.06)	404.58 (±9.89)	−1219.29 (±29.92)	1015.56 (±35.49)	−1656.75 (±67.19)
NC-para	461.02 (±22.27)	−510.35 (±75.35)	482.24 (±10.23)	−1376.47 (±79.80)	1226.57 (±9.20)	−2029.15 (±86.25)
NC-anti	430.91 (±19.96)	−304.87 (±31.85)	435.23 (±6.04)	−1333.24 (±28.48)	1122.47 (±38.34)	−2274.48 (±28.89)
CC-para	431.13 (±19.43)	−328.83 (±53.26)	432.05 (±5.09)	−1332.58 (±28.75)	1120.62 (±38.98)	−2249.10 (±49.46)
CC-anti	405.29 (±19.06)	−455.88 (±80.18)	438.76 (±5.77)	−1326.89 (±28.07)	1102.41 (±36.69)	−2134.19 (±70.23)
nest-para	365.21 (±18.72)	−802.26 (±45.35)	398.71 (±6.37)	−1298.78 (±29.30)	1148.09 (±34.89)	−1799.23 (±35.00)
nest-anti	N/A	N/A	N/A	N/A	N/A	N/A
anti-nest-para	375.69 (±22.01)	−409.77 (±96.34)	417.78 (±5.15)	−1311.05 (±29.57)	1116.50 (±42.58)	−2185.20 (±84.52)
anti-nest-anti	351.90 (±24.82)	−931.58 (±54.50)	383.77 (±9.38)	−1202.00 (±34.97)	1028.69 (±35.68)	−1582.09 (±57.41)

Individual free-energy terms are as defined in Eq. 2. The free-energy unit is kcal/mol. Individual error bars are given in parentheses.

TABLE 4 Individual free-energy terms contributing to the free energy of Aβ-(1–42) dimer conformations ($\langle G_{s,\,vdw}\rangle_A = \langle G_{s,\,vdw,\,6}\rangle_A + \langle G_{s,\,vdw,\,12}\rangle_A$)

Dimers	$\langle U_{m,\,pack}\rangle$	$\langle U_{m,\,coul}\rangle$	$\langle G_{cav}\rangle_A$	$\langle G_{s,\,vdw,\,6}\rangle_A$	$\langle G_{s,\,vdw,\,12}\rangle_A$	$\langle G_{pol}\rangle_A$
NN-para	423.54 (±18.81)	−801.58 (±55.65)	442.64 (±6.43)	−1389.39 (±29.91)	1202.60 (±40.09)	−1872.54 (±55.34)
NN-anti	418.98 (±18.66)	−789.11 (±37.77)	450.74 (±5.11)	−1338.09 (±28.06)	1100.53 (±40.16)	−1786.60 (±35.12)
NC-para	460.80 (±21.73)	−508.38 (±78.92)	482.35 (±9.22)	−1490.08 (±39.94)	1236.89 (±42.65)	−2031.03 (±85.56)
NC-anti	408.67 (±23.29)	−613.37 (±66.99)	443.42 (±8.72)	−1352.46 (±31.52)	1142.00 (±41.93)	−1934.17 (±55.92)
CC-para	557.70 (±25.02)	−307.78 (±61.98)	456.23 (±11.09)	−1356.90 (±44.31)	1130.10 (± 3.64)	−2271.67 (±48.84)
CC-anti	403.06 (±23.78)	−442.91 (±51.25)	435.44 (±8.54)	−1309.01 (±30.90)	1095.78 (±37.15)	−2134.30 (±52.92)
nest-para	412.00 (±19.02)	−397.71 (±45.33)	430.32 (±4.03)	−1372.41 (±29.68)	1200.69 (±36.29)	−2295.16 (±44.52)
nest-anti	386.48 (±19.11)	−788.56 (±55.26)	419.63 (±4.42)	−1314.58 (±31.35)	1143.89 (±38.48)	−1819.24 (±50.32)
anti-nest-para	407.44 (±19.35)	−461.78 (±51.58)	436.99 (±7.16)	−1373.93 (±32.87)	1163.51 (±37.94)	−2112.97 (±58.99)
anti-nest-anti	326.80 (±23.25)	−875.27 (±48.24)	412.45 (±8.93)	−1305.67 (±32.92)	1104.56 (±37.83)	−1556.46 (±55.40)

Individual free-energy terms are as defined in Eq. 2. The free-energy unit is kcal/mol. Individual error bars are given in parentheses.

our coarse-grained model adopts a β-hairpin conformation with a β-turn between Asp-23 and Lys-28. The presence of this β-turn is consistent with a structural model for Aβ fibrils based on solid-state NMR experimental constraints (Petkova et al., 2002). In our model, the β-hairpin monomer conformation is stabilized by intrastrand hydrogen bonds, whereas in the structural model for Aβ fibrils (Petkova et al., 2002) the peptides in a fibril interact by interpeptide hydrogen bonds along the fibrillar axis. An intrastrand salt bridge interaction between Asp-23 and Lys-28 may play a critical role in stability of fibrils (Ma and Nussinov, 2002). In our model, the β-turn is not formed due to any amino acid-specific interactions. Expanding our coarse-grained model to include salt bridge and hydrophobic interactions, which are amino acid-specific, will allow us to model a wider range of oligomeric structures, including the bent double-layered hairpin-like structure observed in experiments (Petkova et al., 2002) and all-atom simulations (Ma and Nussinov, 2002). 3), We show by using all-atom simulations that planar, β-sheet-like dimer conformations, predicted by our model, are in general energetically unfavorable compared to the α-helical monomer conformations in water environment. Moreover, the free-energy comparison of Aβ(1–40) and Aβ(1–42) dimer conformations shows that there is no significant free-energy difference between these two alloforms. 4), Aβ dimer conformations, predicted by the coarse-grained model, do not change drastically during our all-atom simulations, and they yield reasonable conformational free energies, which suggests that our simple coarse-grained model represents a good theoretical base upon which we will be able to develop a more sophisticated model by incorporating amino acid-specific interactions.

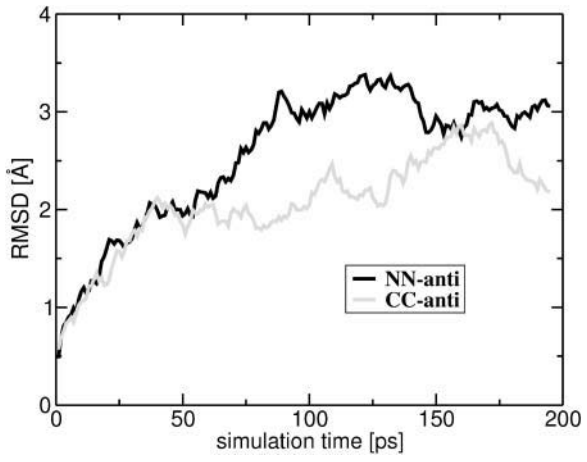

FIGURE 4 Root mean square displacement of two Aβ(1–40) dimer conformations, NN-anti and CC-anti, as a function of time during the production run of all-atom molecular mechanics simulation.

In conclusion, planar β-strand Aβ dimers as predicted by our coarse-grained model cannot account for experimentally observed differences in Aβ oligomer formation between Aβ(1–40) and Aβ(1–42) alloforms (Bitan et al., 2003a). It is not understood yet at which stage of oligomer formation those differences occur and what is the exact mechanism that drives the two alloforms along different pathways. To account for oligomer formation differences between the two Aβ alloforms, our coarse-grained model can be expanded to include other intra- and interpeptide interactions between amino acids, in particular the ones that originate in charge and in hydropathic character of the side chains, the importance of which has been demonstrated recently in vitro (Bitan et al., 2003b,c).

We thank J. Hermans, E. I. Shakhnovich, and D. B. Teplow for valuable advice, discussions, and critical reviews of the manuscript.

This work was supported by the Memory Ride Foundation and Petroleum Research Fund. N.V.D acknowledges the support of University of North Carolina Research Council grant and Muscular Dystrophy Association grant (MDA3702).

REFERENCES

Antzutkin, O. N., J. J. Balbach, and R. Tycko. 2003. Site-specific identification of non-beta-strand conformations in Alzheimer's β-amyloid fibrils by solid-state NMR. *Biophys. J.* 84:3326–3335.

Antzutkin, O. N., R. D. Leapman, J. J. Balbach, and R. Tycko. 2002. Supramolecular structural constraints on Alzheimer's beta-amyloid fibrils from electron microscopy and solid-state nuclear magnetic resonance. *Biochemistry.* 41:15436–15450.

Balbach, J. J., A. T. Petkova, N. A. Oyler, O. N. Antzutkin, D. J. Gordon, S. C. Meredith, and R. Tycko. 2002. Supramolecular structure in full-length Alzheimer's β-amyloid fibrils: evidence for a parallel β-sheet organization from solid-state nuclear magnetic resonance. *Biophys. J.* 83:1205–1216.

Barrow, C. J., A. Yasuda, P. T. M. Kenny, and M. G. Zagorski. 1992. Solution conformations and aggregational properties of synthetic amyloid beta-peptides of Alzheimer's disease. Analysis of circular dichroism spectra. *J. Mol. Biol.* 225:1075–1093.

Barrow, C. J., and M. G. Zagorski. 1991. Solution structures of beta peptide and its constituent fragments: relation to amyloid deposition. *Science.* 253:179–182.

Berendsen, H. J. C., J. P. M. Postma, W. F. van Gunsteren, A. Dinola, and J. R. Haak. 1984. Molecular-dynamics with coupling to an external bath. *J. Chem. Phys.* 81:3684–3690.

Berendsen, H. J. C., J. P. M. Postma, W. F. van Gunsteren, and J. Hermans. 1981. Interaction models for water in relation to protein hydration. *In* Intermolecular Forces. B. Pullman, editor. Reidel, Dordrecht, The Netherlands. 331–342.

Bitan, G., M. D. Kirkitadze, A. Lomakin, S. S. Vollers, G. B. Benedek, and D. B. Teplow. 2003a. Amyloid beta-protein (Ab) assembly: A beta 40 and A beta 42 oligomerize through distinct pathways. *Proc. Natl. Acad. Sci. USA.* 100:330–335.

Bitan, G., A. Lomakin, and D. B. Teplow. 2001. Amyloid-β-protein oligomerization: prenucleation interactions revealed by photo-induced cross-linking of unmodified proteins. *J. Biol. Chem.* 276:35176–35184.

Bitan, G., B. Tarus, S. S. Vollers, H. A. Lashuel, M. M. Condron, J. E. Straub, and D. B. Teplow. 2003b. A molecular switch in amyloid assembly: Met^{35} and amyloid beta-protein oligomerization. *J. Am. Chem. Soc.* 125:15359–15365.

Bitan, G., S. S. Vollers, and D. B. Teplow. 2003c. Elucidation of primary structure elements controlling early amyloid beta-protein oligomerization. *J. Biol. Chem.* 278:34882–34889.

Bonneau, R., and D. Baker. 2001. Ab initio protein structure prediction: progress and prospects. *Annu. Rev. Biophys. Biomol. Struct.* 30:173–189.

Borreguero, J. M., N. V. Dokholyan, S. V. Buldyrev, H. E. Stanley, and E. I. Shakhnovich. 2002. Thermodynamics and folding kinetic analysis of the SH3 domain from discrete molecular dynamics. *J. Mol. Biol.* 318:863–876.

Bucciantini, M., E. Giannoni, F. Chiti, F. Baroni, L. Formigli, J. Zurdo, N. Taddel, G. Ramponi, C. M. Dobson, and M. Stefani. 2002. Inherent toxicity of aggregates implies a common mechanism for protein misfolding diseases. *Nature.* 416:507–511.

Chou, P. Y., and G. D. Fasman. 1974. Prediction of protein conformation. *Biochemistry.* 13:222–245.

Coles, M., W. Bicknell, A. A Watson, D. P. Fairlie, and D. J. Craik. 1998. Solution structure of amyloid-beta peptide (1–40) in a water-micelle environment: is the membrane spanning domain where we think it is? *Biochemistry.* 37:11064–11077.

Creighton, T. E. 1993. Proteins: Structures and Molecular Properties, 2nd ed. Freeman and Co., New York.

Crescenzi, O., S. Tomaselli, R. Guerrini, S. Salvatori, A. M. D'Ursi, P. A. Temussi, and D. Picone. 2002. Solution structure of the Alzheimer amyloid β-peptide (1–42) in an apolar microenvironment: similarity with a virus fusion domain. *Eur. J. Biochem.* 269:5642–5648.

Dahlgren, K. N., A. M. Manelli, W. Blaine Stine, Jr., L. K. Baker, G. A. Krafft, and M. J. LaDu. 2002. Oligomeric and fibrillar species of amyloid-β peptides differentially affect neuronal viability. *J. Biol. Chem.* 277:32046–32053.

Darden, T., D. M. York, and L. G. Pedersen. 1993. Particle mesh Ewald: an N log(N) method for Ewald sums in large systems. *J. Chem. Phys.* 98: 10089–10092.

Dill, K. A. 1999. Polymer principles and protein folding. *Prot. Sci.* 8:1166–1180.

Ding, F., J. M. Borreguero, S. V. Buldyrev, H. E. Stanley, and N. V. Dokholyan. 2003. A mechanism for the α-helix to β-hairpin transition. *Proteins: Structure, Function, and Genetics.* 53:220–228.

Ding, F., N. V. Dokholyan, S. V. Buldyrev, H. E. Stanley, and E. I. Shakhnovich. 2002a. Direct molecular dynamics observation of protein folding transition state ensemble. *Biophys. J.* 83:3525–3532.

Ding, F., N. V. Dokholyan, S. V. Buldyrev, H. E. Stanley, and E. I. Shakhnovich. 2002b. Molecular dynamics simulation of the SH3 domain aggregation suggests a generic amyloidogenesis mechanism. *J. Mol. Biol.* 324:851–857.

Dinner, A. R., S. S. So, and M. Karplus. 2002. Statistical analysis of protein folding kinetics. *In* Advances in Chemical Physics, Vol. 120. Computational Methods for Protein Folding. Richard A. Friesner, editor. Wiley Interscience, Chichester, UK. 1–34.

Dodart, J.-C., K. R. Bales, K. S. Gannon, S. J. Greene, R. B. DeMattos, C. Mathis, C. A. DeLong, S. Wu, W. Wu, D. M. Holtzman, and S. M. Paul. 2002. Immunization reverses memory deficits without reducing brain Aβ burden in Alzheimer's disease model. *Nat. Neurosci.* 5:452–457.

Dokholyan, N. V., S. V. Buldyrev, H. E. Stanley, and E. I. Shakhnovich. 1998. Molecular dynamics studies of folding of a protein-like model. *Fold. Des.* 3:577–587.

Durell, S. R., H. R. Guy, N. Arispe, E. Rojas, and H. B. Pollard. 1994. Theoretical models of the ion channel structure of amyloid β-protein. *Biophys. J.* 67:2137–2145.

El-Agnaf, O. M. A., D. S. Mahil, B. P. Patel, and B. M. Austen. 2000. Oligomerization and toxicity of β-amyloid-42 implicated in Alzheimer's disease. *Biochem. Biophys. Res. Commun.* 273:1003–1007.

El-Agnaf, O. M. A., S. Nagala, B. P. Patel, and B. M. Austen. 2001. Non-fibrillar oligomeric species of the amyloid ABri peptide, implicated in familial British dementia, are more potent at inducing apoptotic cell death than protofibrils or mature fibrils. *J. Mol. Biol.* 310:157–168.

Enya, M., M. Morishima-Kawashima, M. Yoshimura, Y. Shinkai, K. Kusui, K. Khan, D. Games, D. Schenk, S. Sugihara, H. Yamaguchi, and Y. Ihara. 1999. Appearance of sodium dodecyl sulfate-stable amyloid β-protein (Aβ) dimer in the cortex during aging. *Am. J. Pathol.* 154: 271–279.

Ferro, D. R., J. E. McQueen, J. T. McCown, and J. Hermans. 1980. Energy minimization of rubredoxin. *J. Mol. Biol.* 136:1–18.

Fersht, A. R., and V. Daggett. 2002. Protein folding and unfolding at atomic resolution. *Cell.* 108:573–582.

Funato, H., M. Enya, M. Yoshimura, M. Morishima-Kawashima, and Y. Ihara. 1999. Presence of sodium dodecyl sulfate-stable amyloid β-protein dimers in the hippocampus CA1 not exhibiting neurofibrillary tangle formation. *Am. J. Pathol.* 155:23–28.

Garzon-Rodriguez, W., M. Sepulveda-Becerra, S. Milton, and C. G. Glabe. 1997. Soluble amyloid Aβ-(1–40) exists as a stable dimer at low concentrations. *J. Biol. Chem.* 272:21037–21044.

Golde, T. E., C. B. Eckman, and S. G. Younkin. 2000. Biochemical detection of A beta isoforms: implications for pathogenesis, diagnosis, and treatment of Alzheimer's disease. *Biochem. Biophys. Acta.* 1502:172–187.

Gravina, S. A., L. B. Ho, C. B. Eckman, K. E. Long, L. Otvos, Jr., L. H. Younkin, N. Suzuki, and S. G. Younkin. 1995. Amyloid beta protein (A beta) in Alzheimer's disease brain: biochemical and immunocytochemical analysis with antibodies specific for forms ending at A beta 40 or A beta 42(43). *J. Biol. Chem.* 270:7013–7016.

Gursky, O., and S. Aleshkov. 2000. Temperature-dependent β-sheet formation in β-amyloid $A\beta_{1-40}$ peptide in water: uncoupling β-structure folding from aggregation. *Biochim. Biophys. Acta.* 1476:93–102.

Hartley, D. M., D. M. Walsh, C. P. Ye, T. Diehl, S. Vasquez, P. M. Vassilev, D. B. Teplow, and D. J. Selkoe. 1999. Protofibrillar intermediates of amyloid β-protein induce acute electrophysiological changes and progressive neurotoxicity in cortical neurons. *J. Neurosci.* 19:8876–8884.

Hermans, J., H. J. C. Berendsen, W. F. van Gunsteren, and J. P. M. Postma. 1984. A consistent empirical potential for water-protein interactions. *Biopolymers.* 23:1513–1518.

Hermans, J., R. H. Yun, J. Leech, and D. Cavanaugh. 1994. Sigma documentation. University of North Carolina: http://hekto.med.unc.edu:8080/HERMANS/software/SIGMA/index.html.

Hsia, A. Y., E. Masliah, L. McConlogue, G.-Q. Yu, G. Tatsuno, K. Hu, D. Kholodenko, R. C. Malenka, R. A. Nicoll, and L. Mucke. 1999. Plaque-independent disruption of neural circuits in Alzheimer's disease mouse models. *Proc. Natl. Acad. Sci. USA.* 96:3228–3233.

Huang, T. H. J., D.-S. Yang, N. P. Plaskos, S. Go, C. M. Yip, P. E. Fraser, and A. Chakrabartty. 2000. Structural studies of soluble oligomers of Alzheimer β-amyloid peptide. *J. Mol. Biol.* 297:73–87.

Humphrey, W., A. Dalke, and K. Schulten. 1996. VMD: visual molecular dynamics. *J. Mol. Graphics.* 14.1:33–38.

Iwatsubo, T., A. Odaka, N. Suzuki, H. Mizusawa, N. Nukina, and Y. Ihara. 1994. Visualization of A beta 42(43) and A beta 40 in senile plaques with end-specific A beta monoclonals: evidence that an initially deposited species is A beta 42(43). *Neuron.* 13:45–53.

Karplus, M., and J. A. McCammon. 2002. Molecular dynamics simulations of biomolecules. *Nat. Struct. Biol.* 9:646–652.

Kayed, R., E. Head, J. L. Thompson, T. M. McIntire, S. C. Milton, C. W. Cotman, and C. G. Glabe. 2003. Common structure of soluble amyloid oligomers implies common mechanisms of pathogenesis. *Science.* 300:486–489.

Kirkitadze, M. D., G. Bitan, and D. B. Teplow. 2002. Paradigm shifts in Alzheimer's disease and other neurodegenerative disorders: the emerging role of oligomeric assemblies. *J. Neurosci. Res.* 69:567–577.

Kirkitadze, M. D., M. M. Condron, and D. B. Teplow. 2001. Identification and characterization of key kinetic intermediates in amyloid b-protein fibrillogenesis. *J. Mol. Biol.* 312:1103–1119.

Klein, W. L. 2002a. Aβ toxicity in Alzheimer's disease: globular oligomers (ADDLs) as new vaccine and drug targets. *Neurochem. Int.* 41:345–352.

Klein, W. L. 2002b. ADDLs and protofibrils—the missing link? *Neurobiol. Aging.* 23:231–233.

Klein, W. L., G. A. Krafft, and C. E. Finch. 2001. Targeting small A beta oligomers: the solution to an Alzheimer's disease conundrum? *Trends Neurosci.* 24:219–224.

Kuo, Y.-M., M. R. Emmerling, C. Vigo-Pelfrey, T. C. Kasunic, J. B. Kirkpatrick, G. H. Murdoch, M. J. Ball, and A. E. Roher. 1996. Water-soluble Aβ (N-40, N-42) oligomers in normal and Alzheimer disease brains. *J. Biol. Chem.* 271:4077–4081.

Kuo, Y.-M., S. Webster, M. R. Emmerling, N. De Lima, and A. E. Roher. 1998. Irreversible dimerization/tetramerization and post-translational modifications inhibit proteolytic degradation of A-β peptides of Alzheimer's disease. *Biochim. Biophys. Acta.* 1406:291–298.

Lambert, M. P., A. K. Barlow, B. A Chromy, C. Edwards, R. Freed, M. Liosatos, T. E. Morgan, I. Rozovsky, B. Trommer, K. L. Viola, P. Wals, C. Zhang, C. E. Finch, G. A. Krafft, and W. L. Klein. 1998. Diffusible, nonfibrillar ligands derived from Ab(1–42) are potent central nervous system neurotoxins. *Proc. Natl. Acad. Sci USA.* 95:6448–6453.

Leach, A. R. 2001. Molecular Modelling: Principles and Applications, 2nd ed. Prentice-Hall, New York.

Levitt, M., M. Gerstein, E. Huang, S. Subbiah, and J. Tsai. 1997. Protein folding: the endgame. *Annu. Rev. Biochem.* 66:549–579.

Ma, B., and R. Nussinov. 2002. Stabilities and conformations of Alzheimer's β-amyloid peptide oligomers (Aβ_{16-22}, Aβ_{16-35}, and Aβ_{10-35}): Sequence effects. *Proc. Natl. Acad. Sci. USA.* 99:14126–14131.

Malinchik, S. B., H. Inouye, K. E. Szumowski, and D. A. Kirschner. 1998. Structural analysis of Alzheimer's β(1–40) amyloid: protofilament assembly of tubular fibrils. *Biophys. J.* 74:537–545.

Mendes, J., R. Guerois, and L. Serrano. 2002. Energy estimation in protein design. *Curr. Opin. Struct. Biol.* 12:441–446.

Mirny, L., and E. I. Shakhnovich. 2001. Protein folding theory: from lattice to all-atom models. *Annu. Rev. Biophphys. Biomol. Struct.* 30:361–396.

Mucke, L., E. Masliah, G.-Q. Yu, M. Mallory, E. M. Rockenstein, G. Tatsuno, K. Hu, D. Kholodenko, K. Johnson-Wood, and L. McConlogue. 2000. High-level neuronal expression of Aβ-(1–42) in wild-type human amyloid protein precursor transgenic mice: synaptotoxicity without plaque formation. *J. Neurosci.* 20:4050–4058.

Nilsberth, C., A. Westlind-Danielsson, C. B. Eckman, M. M. Condron, K. Axelman, C. Forsell, C. Stenh, J. Luthman, D. B. Teplow, S. G. Younkin, J. Näslund, and L. Lannfelt. 2001. The 'Arctic' APP mutation (E693G) causes Alzheimer's disease by enhanced Aβ protofibril formation. *Nat. Neurosci.* 4:887–893.

Petkova, A. T., Y. Ishii, J. J. Balbach, O. N. Antzutkin, R. D. Leapman, F. Delaglio, and R. Tycko. 2002. A structural model for Alzheimer's β-amyloid fibrils based on experimental constraints from solid state NMR. *Proc. Natl. Acad. Sci. USA.* 99:16742–16747.

Plotkin, S. S., and J. N. Onuchic. 2002. Understanding protein folding with energy landscape theory, Part I: basic concepts. *Q. Rev. Biophys.* 35:111–167.

Podlisny, M. B., B. L. Ostaszewski, S. L. Squazzo, E. H. Koo, R. E. Rydell, D. B. Teplow, and D. J. Selkoe. 1995. Aggregation of secreted amyloid β-protein into sodium dodecyl sulfate-stable oligomers in cell culture. *J. Biol. Chem.* 270:9564–9570.

Podlisny, M. B., D. M. Walsh, P. Amarante, B. L. Ostaszewski, E. R. Stimson, J. E. Maggio, D. B. Teplow, and D. J. Selkoe. 1998. Oligomerization of endogenous and synthetic amyloid β-protein at nanomolar levels in cell culture and stabilization of monomer by Congo red. *Biochemistry.* 37:3602–3611.

Rapaport, D. C. 1997. The Art of Molecular Dynamics Simulation. Cambridge University Press, Cambridge, UK.

Roher, A. E., M. O. Chaney, Y.-M. Kuo, S. D. Webster, W. B. Stine, L. J. Haverkamp, A. S. Woods, R. J. Cotter, J. M. Tuohy, G. A. Krafft, B. S. Bonnell, and M. R. Emmerling. 1996. Morphology and toxicity of Aβ dimer derived from neuritic and vascular amyloid deposits of Alzheimer's disease. *J. Biol. Chem.* 271:20631–20635.

Scheuner, D., C. Eckman, M. Jensen, X. Song, M. Citron, N. Suzuki, T. D. Bird, J. Hardy, M. Hutton, W. Kukull, E. Larson, E. LevyLahad, M. Viitanen, E. Peskind, P. Poorkaj, G. Schellenberg, R. Tanzi, W. Wasco, L. Lannfelt, D. Selkoe, and S. Younkin. 1996. Secreted amyloid beta-protein similar to that in the senile plaques of Alzheimer's disease is increased in vivo by the presenilin 1 and 2 and APP mutations linked to familial Alzheimer's disease. *Nat. Med.* 2:864–870.

Selkoe, D. J. 1997. Alzheimer's disease: genotypes, phenotypes and treatments. *Science.* 275:630–631.

Serpell, L. C., C. C. F. Blake, and P. E. Fraser. 2000. Molecular structure of a fibrillar Alzheimer's Aβ fragment. *Biochemistry.* 39:13269–13275.

Shen, C. L. S., and M. Murphy. 1995. Solvent effects on self-assembly of beta-amyloid peptide. *Biophys. J.* 69:640–651.

Smith, A. V., and C. K. Hall. 2001a. α-Helix formation: discontinuous molecular dynamics on an intermediate-resolution protein model. *Proteins.* 4:344–360.

Smith, A. V., and C. K. Hall. 2001b. Protein refolding versus aggregation: computer simulations on an intermediate-resolution protein model. *J. Mol. Biol.* 312:187–202.

Snow, C. D., N. Nguyen, V. S. Pande, and M. Gruebele. 2002. Absolute comparison of simulated and experimental protein-folding dynamics. *Nature.* 420:102–106.

Soreghan, B., J. Kosmoski, and C. Glabe. 1994. Surfactant properties of Alzheimer's Aβ peptides and the mechanism of amyloid aggregation. *J. Biol. Chem.* 269:28551–28554.

Suzuki, N., T. T. Cheung, X.-D. Cai, A. Odaka, L. Otvos, Jr., C. Eckman, T. E. Golde, and S. G. Younkin. 1994. An increased percentage of long amyloid beta protein secreted by familial amyloid beta protein precursor (beta APP717) mutants. *Science.* 264:1336–1340.

Takada, S., Z. Luthey-Schulten, and P. G. Wolynes. 1999. Folding dynamics with nonadditive forces: a simulation study of a designer helical protein and a random heteropolymer. *J. Chem. Phys.* 110:11616–11629.

Thirumalai, D., D. K. Klimov, and R. I. Dima. 2002. Insights into specific problems in protein folding using simple concepts. *In* Advances in Chemical Physics, Vol. 120. Computational Methods for Protein

Folding. Richard A. Friesner, editor. Wiley Interscience, Chichester, UK. 35–76.

Thompson, L. K. 2003. Unraveling the secrets of Alzheimer's β-amyloid fibrils. *Proc. Natl. Acad. Sci. USA.* 100:383–385.

Tjernberg, L. O., D. J. E. Callaway, A. Tjernberg, S. Hahne, C. Lilliehöök, L. Terenius, J. Thyberg, and C. Nordstedt. 1999. A molecular model of Alzheimer amyloid β-peptide fibril formation. *J. Biol. Chem.* 274: 12619–12625.

Tjernberg, L. O., A. Tjernberg, N. Bark, Y. Shi, B. P. Ruzsicska, Z. Bu, J. Thyberg, and D. J. E. Callaway. 2002. Assembling amyloid fibrils from designed structures containing a significant amyloid β-peptide fragment. *Biochem. J.* 366:343–351.

Török, M., S. Milton, R. Kayed, P. Wu, T. McIntire, C. G. Glabe, and R. Langen. 2002. Structural and dynamic features of Alzheimer's Aβ peptide in amyloid fibrils studied by site-directed spin labeling. *J. Biol. Chem.* 277:40810–40815.

Vorobjev, Y. N., J. C. Almagro, and J. Hermans. 1998. Discrimination between native and intentionally misfolded conformations of proteins: ES/IS, a new method for calculating conformational free energy that uses both dynamics simulations with an explicit solvent and an implicit solvent continuum model. *Proteins.* 32:399–413.

Vorobjev, Y. N., and J. Hermans. 1999. ES/IS: estimation of conformational free energy by combining dynamics simulations with explicit solvent with an implicit solvent continuum model. *Biophys. Chem.* 78: 195–205.

Vorobjev, Y. N., and J. Hermans. 2001. Free energies of protein decoys provide insight into determinants of protein stability. *Protein Sci.* 10: 2498–2506.

Walsh, D. M., D. M. Hartley, Y. Kusumoto, Y. Fezoui, M. M. Condron, A. Lomakin, G. B. Benedek, D. J. Selkoe, and D. B. Teplow. 1999. Amyloid β-protein fibrillogenesis: structure and biological activity of protofibrillar intermediates. *J. Biol. Chem.* 274:25945–25952.

Walsh, D. M., I. Klyubin, J. V. Fadeeva, W. K. Cullen, R. Anwyl, M. S. Wolfe, M. J. Rowan, and D. J. Selkoe. 2002. Naturally secreted oligomers of amyloid b protein potently inhibit hippocampal long-term potentiation *in vivo*. *Nature*. 416:535–539.

Walsh, D. M., A. Lomakin, G. B. Benedek, M. M. Condron, and D. Teplow. 1997. Amyloid β-protein fibrillogenesis: detection of a protofibrillar intermediate. *J. Biol. Chem.* 272:22364–22372.

Weggen, S., J. L. Ericksen, P. Das, S. A. Sagi, R. Wang, C. U. Pietrzik, K. A. Findlay, T. W. Smith, M. P. Murphy, T. Butler, D. E. Kang, N. Marquez-Sterling, T. E. Golde, and E. H. Koo. 2001. A subset of NSAIDs lower amyloidogenic A beta 42 independently of cyclooxygenase activity. *Nature*. 414:212–216.

Westerman, M. A., D. Cooper-Blacketer, A. Mariash, L. Kotilinek, T. Kawarabayashi, L. H. Younkin, G. A. Carlson, S. G. Younkin, and K. H. Ashe. 2002. The relationship between Ab and memory in the Tg2576 mouse model of Alzheimer's disease. *J. Neurosci.* 22:1858–1867.

Wolynes, P. G., Z. Luthey-Schulten, and J. N. Onuchic. 1996. Fast folding experiments and the topography of protein folding energy landscapes. *Chem. Biol.* 3:425–432.

Xia, W., J. Zhang, D. Kholodenko, M. Citron, M. B. Podlisny, D. B. Teplow, C. Haass, P. Seubert, E. H. Koo, and D. J. Selkoe. 1995. Enhanced production and oligomerization of the 42-residue amyloid β-protein by Chinese hampster ovary cells stably expressing mutant presinilins. *J. Biol. Chem.* 272:7977–7982.

Yankner, B. A. 1996. Mechanisms of neuronal degeneration in Alzheimer's disease. *Neuron.* 16:921–932.

Yong, W., A. Lomakin, M. D. Kirkitadze, D. B. Teplow, S.-H. Chen, and G. B. Benedek. 2002. Structure determination of micelle-like intermediates in amyloid b-protein fibril assembly by using small angle neutron scattering. *Proc. Natl. Acad. Sci. USA.* 99:150–154.

Zagorski, M. G., and C. J. Barrow. 1992. NMR studies of amyloid beta-peptides: proton assignments, secondary structure, and mechanism of an alpha-helix—beta-sheet conversion for a homologous, 28-residue, N-terminal fragment. *Biochemistry.* 31:5621–5631.

Zagrovic, B., C. D. Snow, M. R. Shirts, and V. S. Pande. 2002. Simulation of folding of a small α-helical protein in atomistic detail using worldwide-distributed computing. *J. Mol. Biol.* 323:927–937.

Zhou, Y., and M. Karplus. 1997. Folding thermodynamics of a three-helix-bundle protein. *Proc. Natl. Acad. Sci. USA.* 94:14429–14432.